An investigation into the role of Arf6 in MCH-mediated rearrangements in 3T3-L1 preadipocytes

A Senior Honors Thesis

Submitted in Partial Fulfillment of the Requirements for Graduation in the Honors College

By

Bohdan Smich

Biology Major

The College at Brockport

May 13, 2020

Thesis director: Dr. Laurie B. Cook, Professor, Biology

Table of Contents

Abstract

Obesity has become a pandemic in our society. One potential method to alleviate this crisis is the use of pharmaceutical therapy to manage how our bodies metabolize the energy that we consume. Chronic overconsumption can lead to the activation of inflammatory responses and metabolic dysregulation, such as insulin resistance, and promote the obese condition. The pathways involved in the motility of pre-adipocyte cells are important in understanding how our bodies interpret and react to specific biochemical signals. This research is focused on a pathway that activates the expansion and migration of pre-adipocytes. Melanin-concentrating Hormone (MCH) is a neuropeptide that is known for regulating appetite and metabolism within adipocytes through the G protein-coupled receptor, MCHR1. MCHR1 is known to act through a Gq/PLC pathway to destabilize actin. Our proposed pathway is that MCHR1 activates ARNO, a guanine nucleotide exchange factor that is required in the subsequent activation of ADP-ribosylation factor 6 (Arf6). These events in succession may result in destabilized actin in murine 3T3-L1 pre-adipocytes. A pharmaceutical inhibitor of Arf6, NAV-2729, as well as the overexpression of dominant negative ARNO/Arf6 plasmids were used to determine if Arf6 was indeed a downstream signaling component in this pathway. Fluorescence microscopy was used to visualize the actin stress fibers and morphology of the cell and a scratch wound was performed to determine if the migration rate was affected. Preliminary results from our fluorescence stain show that the structure of actin was affected by NAV-2729 after MCH addition, however, additional trials and analysis are required.

Introduction

Melanin-concentrating hormone (MCH) is a hypothalamic neuropeptide that has been shown to play a significant role in the regulation of many mammalian physiological processes including mood, the circadian rhythm, immune responses and metabolism. MCH was recently reported to affect the actin morphology and increase migration rate of and 3T3-L1 preadipocytes [1]. MCH is responsible for eliciting a physiological response via two Melanin-concentrating hormone receptors, MCHR1 and MCHR2. In an experiment carried out by Ludwig et al., when mice were injected with MCH they expressed an increased level of feeding, weight gain, and insulin resistance. Conversely, upon ablation of MCH, the mice began to express leaner phenotypes as a result of their increased metabolic rate and hypophagia [2]. This metabolic response is of interest to the biomedical community due to the continuously worsening obesity epidemic seen throughout the world. Obesity is the result of overconsumption or increased metabolic intake without increased metabolic need that results in elevated levels of adipose tissue. Obesity, if left untreated, has been shown to increase risk of cardiovascular diseases, diabetes, and other chronic conditions such as sleep apnea, liver and kidney diseases and depression. The mechanisms by which MCH may affect appetite are still unclear, however a correlation was found between cases of extreme childhood obesity and mutations in MCHR2 [3]. This correlation points to a potential link between MCH and its role in regulating adipocyte expansion and migration. Adipose tissue is involved in the regulation of appetite via secretion of regulatory hormones such as insulin, adiponectin, and leptin. These hormones function to maintain metabolic homeostasis by providing information about the metabolic state of the body to the brain [1]. Further exploration

into the signaling pathways involved in adipocyte development could be of interest in creating pharmaceutical drugs in an effort to alleviate obesity.

Melanin-concentrating hormone receptors, MCHR1 and MCHR2, belong to a large and highly diverse family of receptors called G protein-coupled receptors (GPCRs) that are encoded by over 800 separate human genes. GPCRs are characterized by their 7 transmembrane alpha helices and are responsible for transmitting a variety of signals from the extracellular environment as well as aiding in the regulation of many cellular signaling pathways. As a result, GPCRs are often targeted by pharmaceutical companies for the purpose of drug therapy. Inactive GPCRs are found bound to a heterotrimeric G protein complex that consists of a GDP-bound G_α monomer and a $G_{\beta\gamma}$ heterodimer. Upon the binding of an agonist, a conformational change results in the receptor assuming its active conformation. The G_α subunit then exchanges its GDP for GTP with the help of a guanine nucleotide-exchange factor (GEF) and dissociates from the $G_{\beta\gamma}$ subunits. Both subunits, now activated, can be used to induce an intracellular response in downstream signaling pathways via second messengers.

ADP-ribosylation factors (Arfs) belong to a family of Ras-related GTP-binding proteins that are known to play a role in the regulation of membrane structure [5,6]. Arf6 inhibition has been shown to diminish cell motility and adhesion in HeLa cells [5]. Cell motility is mediated by a complex mechanism that is dependent on the cell's ability to regulate its membrane composition [8]. Arfs act as molecular switches in being converted to their active GTP-bound state by guanine nucleotide exchange factors (GEFs) and back to their inactive GDP-bound state with the aid of GTPase activating proteins. Once active, Arf6 has the ability to interact with and activate other intracellular macromolecules. ARNO is one of the known GEFs that is responsible for the activation of Arf6 [9]. Arrestins, such as β-arrestin, are adaptor proteins that bind to GPCRs to

inhibit further signaling and promote receptor internalization as well as functioning independently by generating their own signals and regulating other intracellular enzymes [8,10]. Arf6 has been shown to complex with ARNO and β-arrestin to regulate the endocytosis of membrane proteins, such as GLUT4, as well as other membrane-related pathways which are involved in cytoskeletal rearrangements and cell motility [1,7,8]. This leads us to believe that Arf6 may play a critical role in the regulation of adipocyte expansion and motility in 3T3-L1 pre-adipocytes through ARNO and Arf6 via MCH. The role of Arf6 in adipocyte development has been shown previously in other studies, specifically Arf6-mediated lipolysis in which fats are hydrolyzed to fatty acids. In an experiment conducted by Yingqiu Liu et al., a link between increased Arf6 levels and obesity in 3T3-L1 adipocytes was found using RNA interference (RNAi). Their results showed a significant increase in Arf6 levels in the white adipose tissue of older mice and obese (*ob/ob)* mice. Arf6 appeared to play a role in lipolytic activity directly associated with the activation of β-adrenergic receptors [11].

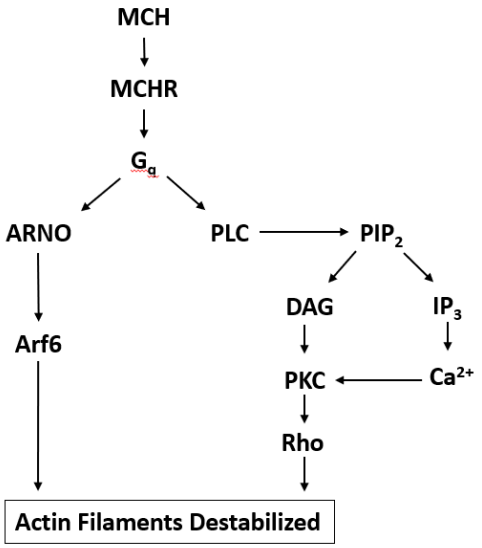

Figure 2. Proposed mechanism for MCH-mediated actin rearrangements in 3T3-L1 preadipocytes. G_q is the G protein alpha subunit responsible for PLC activation. Left: ARNO – GTPase, ADP ribosylation factor 6 (Arf6) Right: Phospholipase C (PLC), Phosphatidylinositol 4,5-bisphosphate (PIP_2), Diacyl glycerol (DAG), Inositol triphosphate (IP_3), Calcium ion (Ca^{2+}), Protein kinase C (PKC) Rho – GTPase.

For our lab in particular, we are interested in the mechanisms by which MCH elicits the expansion and migration of 3T3-L1 preadipocytes. The 3T3-L1 cells are murine adipose stem cells that are widely used in biological research on the development of adipose tissue. Little is known about the downstream signaling components of MCHR1. Two potential mechanisms by which MCH may be responsible for mediating actin rearrangements within 3T3-L1 preadipocytes are phospholipase-C (PLC) activation and activation of ADP-ribosylation factor 6 (Arf6), shown in Figure 2. It has been shown that PLC activation in preadipocytes leads to a decrease in fibroblast morphology [1]. PLC can be activated by the βγ subunits of G proteins to initiate a signaling cascade shown on the right side of figure 2. PLC goes on to hydrolyze PIP_2 to two secondary messengers: IP_3 and DAG. DAG remains within the cell membrane where it recruits Protein kinase C. IP_3 results in the activation of Ca^{2+} channels located on intracellular organelles such as the endoplasmic reticulum resulting in the release of Ca^{2+} into the cytoplasm [1,12,13]. DAG and Ca^{2+}

can both activate PKC which catalyzes the phosphorylation of other intracellular signaling molecules such as Rho. Rho proteins are a family of GTPases which are known for regulating the intracellular cytoskeleton and actin [1,14]. Our goal was to determine if ARNO and Arf6 play a secondary role in this process by Arf6 inactivation. It was hypothesized that if ARNO/Arf6 were effectively inhibited, then we would see a destabilization and as well as a decrease in migration rate. Our first method to determining if Arf6 plays a role in destabilizing actin rearrangements was to use a pharmaceutical inhibitor, NAV-2729, purchased from Tocris. NAV-2729 targets the Arf6 GEF-binding region to effectively inhibit its ability to bind GTP and activate downstream effectors. The second method involved plasmid overexpression of dominant negative, or inactive, forms of ARNO and Arf6 resulting in competitive inhibition of endogenous ARNO/Arf6. The fluorescence stain and scratch wound performed by Cook et al. were repeated with the addition of these two methods. If successful, this research would provide insight into new pathways involved in MCH signaling regulation of the cytoskeleton

Materials and Methods

Cell culture **-** The adherent murine 3T3-L1 cell line was cultured in DMEM media (source) with 10% (v/v) BCS in 250ml culture flasks. The cells were routinely passaged at approximately 80% confluency. The culture media was aspirated before incubation with 5ml of 0.25% trypsin-EDTA until cells balled up but before complete detachment. The trypsin was aspirated, and the flask was rinsed 4 to 5 times with 10ml of culture media. Flasks were inspected under a microscope to verify that the cells were in the media and had not been aspirated with the trypsin-EDTA. A 0.5ml aliquot of the cell suspension was then added to a 250ml culture flask containing 10ml of prewarmed culture media. The flask was placed on a level surface in a static incubator set to 37°C, 20% humidity, and 5% CO_2. The cells were maintained for up to 15 passages.

Approach 1: Pharmaceutical Inhibition of Arf6 using NAV-2729

Scratch Wound **-** Cells were grown to confluency in 60mm culture dishes containing 4ml of culture media. Each plate was labelled with a thin sharpie as shown in Appendix I for reference points to obtain the same field during imaging. The cells were serum starved using DMEM-media for 1 hour and then pre-treated with 10uM NAV-2729 in DMEM-media for an additional hour. The control was left untreated with NAV-2927. The cell monolayer was scratched with a p200 pipette tip. The plates were treated with 1uM MCH and the scratch photographed under a microscope using the method outlined in Appendix I at 3 separate positions on adjacent to the marked lines. The scratch was then photographed every 30 minutes afterwards and the images analyzed using ImageJ software.

Fluorescence stain **-** Cells were grown to 50-60% confluency on 25mm glass coverslips in 30mm culture dishes containing 1ml of culture media. The cells were serum starved in DMEM-media for

1 hour and then pre-treated with 10uM NAV-2729 in DMEM-media for an additional hour. A set of 4 dishes were treated with 1uM MCH and returned to the incubator for 2, 5, and 10 minutes with the control receiving no treatment. The dishes were then immediately transferred to a metal tray on ice and the treatment media aspirated. Each dish was rinsed 2X with 2ml of ice-cold PBS and aspirated. The cells were then fixed with 1ml of 4% Paraformaldehyde (PF) on the benchtop for 10 minutes. The PF was recovered, each place rinsed 3X with 2ml PBS, then washed for 10 minutes with 2ml PBS-T while rocking. Each coverslip was moved onto parafilm in a humidified chamber and 0.25ml of stain (1:100 DAPI, 1:50 Alexa fluor Phalloidin, PBS-T) was dripped onto each coverslip. The coverslips were allowed to sit in the dark for 20 minutes. The coverslips were moved back to their dishes and washed 3X for 5 minutes each while rocking with PBS-T while covered in foil. The dishes were then washed for 5 minutes in PBS while rocking followed by a quick rinse with dH_2O. The coverslips were then transferred to coverslips and mounted using Prolong Gold antifade reagent and sealed using clear nail polish. The slides were allowed to cure for 24 hours prior to viewing with Zeiss AxioCam and AxioVision software.

Approach 2: Competitive inhibition of Arf6 via overexpression of Arf6 DN Plasmid

Bacterial Transformation – Thomas Roberts generously gifted two plasmids: pcDNA3 HA Arf6 (Addgene plasmid # 10834 ; http://n2t.net/addgene:10834 ; RRID:Addgene_10834) contained the gene for wildtype (WT) human Arf6 and pcDNA3 HA Arf6 DN T27N (Addgene plasmid # 10831 ; http://n2t.net/addgene:10831 ; RRID:Addgene_10831) contained a gene for a dominant negative form of human Arf6 (Figure 3). Jim Casanova at University of Virginia graciously gifted two additional plasmids: GFP ARNO containing a gene for WT ARNO as well as GFP ARNO E156K containing a gene for an inactive form of ARNO. The plasmids were used to transform chemically competent *E. coli* (DH5α) using a heat shock protocol from Addgene. The cells were plated on LB agar plates and incubated overnight at 37°C. The resulting colonies were then plated onto LB agar plates containing an appropriate antibiotic; ampicillin for Arf6 plasmids and kanamycin for ARNO plasmids. A ThermoFisher GeneJET Plasmid DNA Miniprep Kit was used to amplify and isolate the plasmids for later use. The isolated plasmids were stored in microfuge tubes at -20°C.

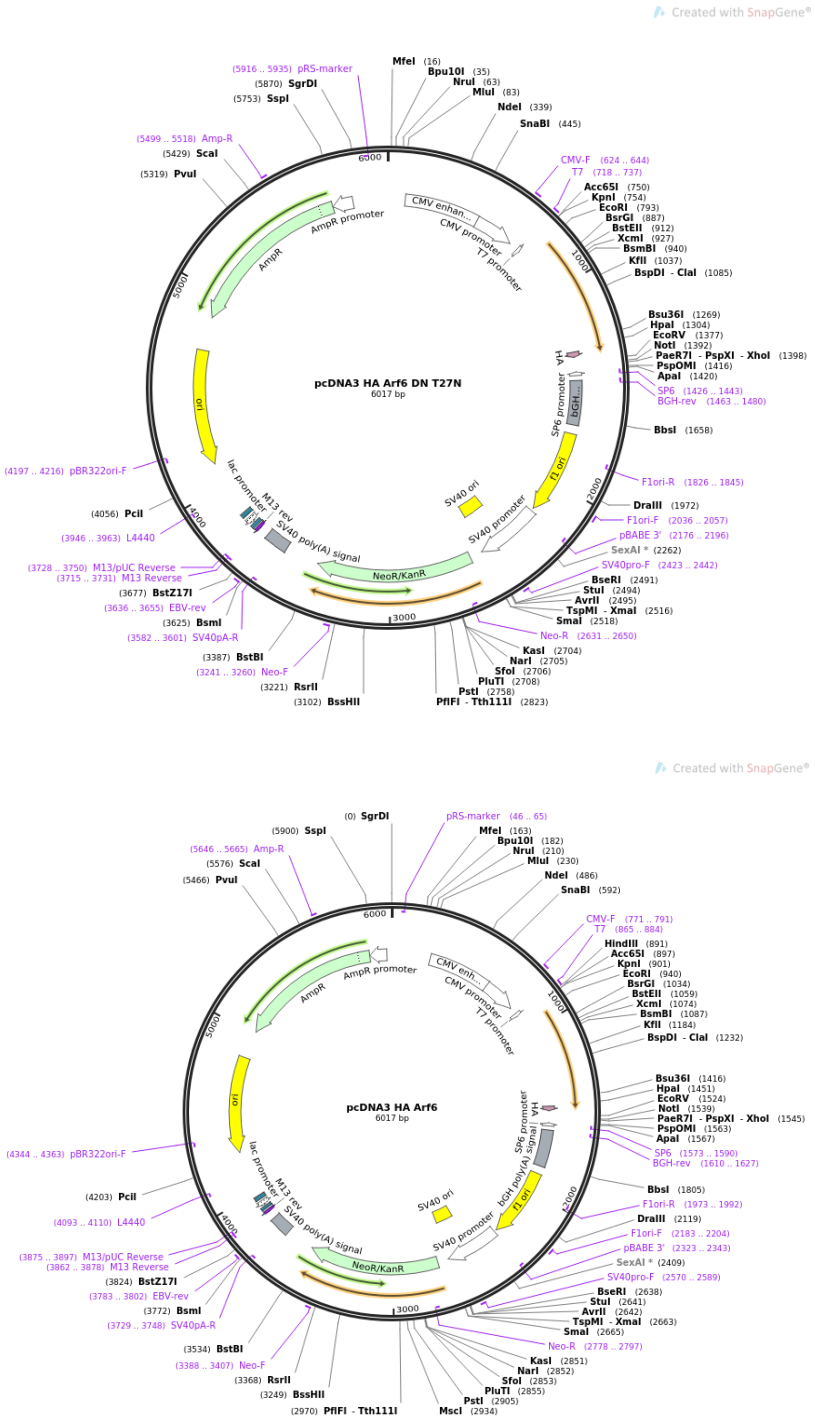

Figure 3. Arf6 DN (Top) and WT Arf6 (Bottom) Plasmid Backbones. The vector backbones of both plasmids, provided by Addgene, were used to determine restriction sites, ECORI and NotI, to be used to verify the plasmids via a double restriction digest (Table 1). Both plasmids contained genes for ampicillin resistance used in antibiotic selection of transformed DH5α *E. coli.*

Restriction Digest – The Arf6 plasmid backbones (above) were used to determine two restriction sites to be used in a double restriction digest. ECORI and NotI were selected based on available restriction enzymes. Buffer compatibility was determined using the Thermo Scientific Conventional Restriction Enzymes Buffer Activity Chart to ensure adequate enzyme activity and to reduce star activity. Each microfuge tube was loaded with 5ul of plasmid from the miniprep, 2ul of 10X buffer, and 1ul of each enzyme. The total volume was brought up to 20ul with dH_2O. The microfuge tubes were incubated in a 37°C water bath for 1 hour and then 4ul of 6X loading dye was added to each. The first well of a 1% TBE agarose gel containing 0.5ug/ml ethidium bromide was loaded with 10ul of a GeneRuler 1Kb DNA Ladder and then 10ul of each digested plasmid was added to the subsequent wells as shown in Table 1. The gel was run at 100V for approximately 1 hour or until the furthest band had reached ~70% of the total gel length. The gel was then viewed under a UV lamp and photographed (Appendix II)

Results

Fluorescence stain cell counts – After completion of the fluorescence stain protocol, slides were blinded by covering identifying information with tape. Each trial was performed in duplicate and 200 cells were counted for each treatment. The cells were classified into three categories: Class A, B, and C, as shown in figure 4C. Class A showed fibroblast-like morphology with prominent actin stress fibers. Class B showed an intermediate morphology with little-to-no actin stress fibers and some protrusions. Class C showed a small round morphology with no stress fibers. Any cells that did not fall distinctly into class A or C were classified as Class B or intermediate. Figure 4 shows cell morphology percentages of cells upon treatment of MCH for intervals of 2, 5, and 10 minutes, with 0 minutes receiving no MCH and serving as the control. Figure 4A shows cell morphology percentages using equal parts DMSO used in the dilution of NAV as a base of comparison to determine the effects of the DMSO vehicle as compared to the NAV drug itself. In this figure, a decrease of 14.95% is seen from no treatment to 10 minutes of MCH treatment as well as a 15.12% increase in fibroblast-like morphology. There does not appear to be any noticeable trend at 2 and 5 minutes as well as with the small round morphology. Figure 4B shows the morphology percentages of NAV-treated cells with MCH addition. A decrease of 15.21% is shown in the intermediate cell morphology from no treatment of MCH to 10 minutes of MCH treatment. There is also an increase of 12.71% in the fibroblast-like phenotype when comparing cells untreated with MCH to cells treated with MCH for 10 minutes. An increase in the small round morphology of 4.29% is seen from 0 to 5 minutes along with a subsequent decrease of 1.79%.

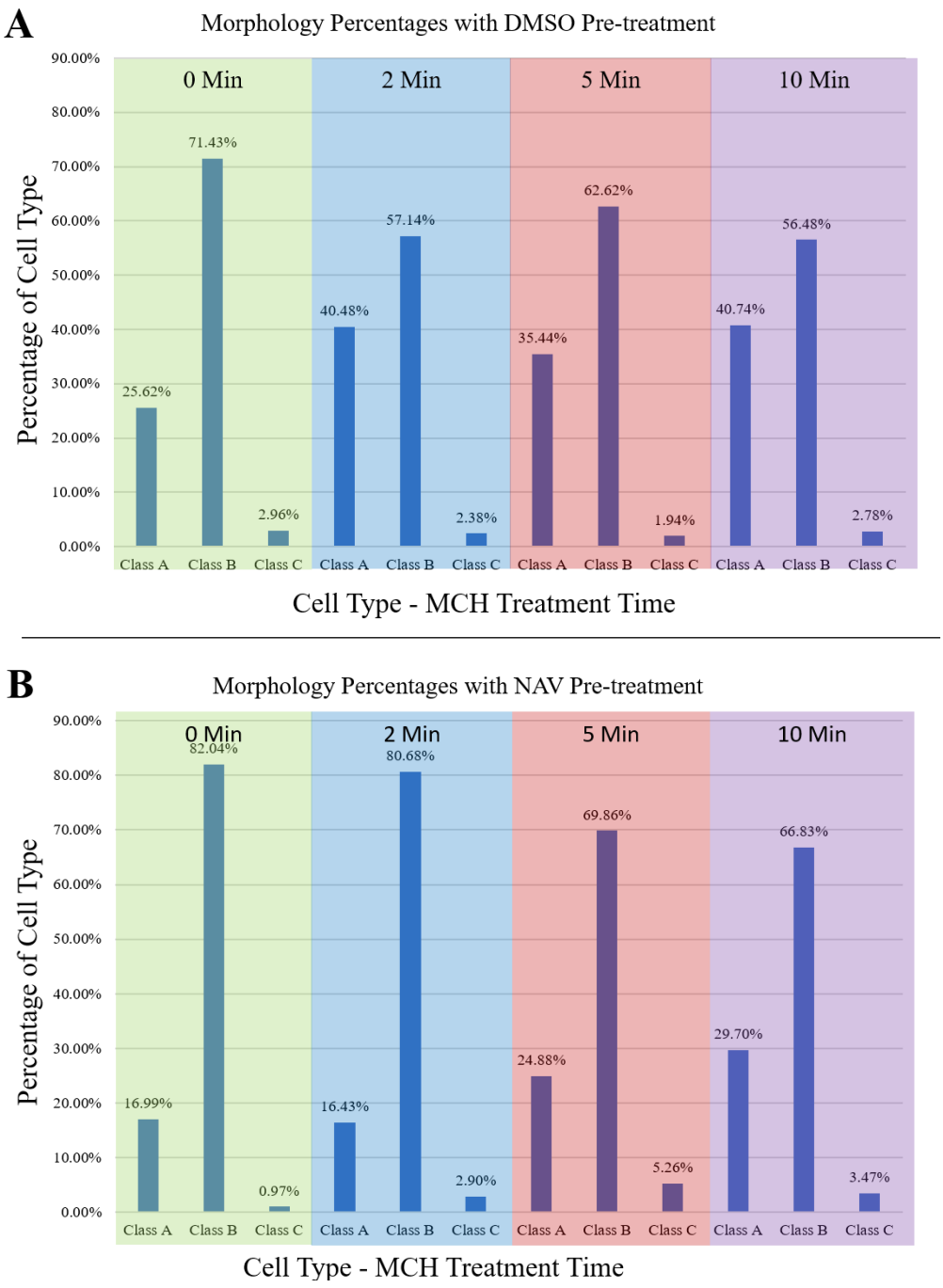

Figure 4. Results from Actin Fluorescent stain with NAV-2729 and DMSO pre-treatments. **(C)** After allowing the slides to cure, 200 cells on each slide were graded as follows: Class A - *Fibroblast with prominent actin stress fibers,* Class B - *Intermediate with few or no stress fibers and some protrusions, or* Class C - *Small Round with no stress fibers and rounded cell morphology*. In both trials, cells were treated with MCH for 2, 5, and 10 minutes as well as being left untreated (0 minutes). **(A)** shows the cell counts pre-treated with DMSO: the vehicle used to dissolve NAV-2729. **(B)** shows the resulting cell counts of NAV-2729 pre-treated slides.

Verification of WT Arf6 and Arf6 DN Plasmids – Each plasmid was digested with ECORI, NotI and HindIII to verify that the restriction sites were present. The bands produced on the agarose gel are shown in Appendix II. The DNA ladder was measured to produce a standard curve and generate an equation for the line of best fit to determine the relative sizes of the resulting bands, shown in Table 1. The plasmid backbones, as shown in Figure 3, both contain restriction sites for ECORI and NotI. Lanes 4-6 and 10-12, in Table 1, showed resulting fragments at approximately 6000bp that indicate a successful single digest. The bands seen in lanes 3 and 9 are consistent with supercoiled uncut DNA plasmid. The secondary fragments in lanes 7 and 13, as a result of the double digest with ECORI and NotI, were calculated to be 627 bp and 654 bp, respectively. These are consistent with the theoretical lengths of 599bp calculated from the plasmid backbones.

Lanes	**1**	**3**	**4**	**5**	**6**	**7**	**9**	**10**	**11**	**12**	**13**
Plasmid	1Kb DNA Ladder	pcDNA3 Arf6 DN T27N (MUT)					pcDNA3 HA Arf6 (WT)				
Restriction Enzyme		-	EcoRI	NotI	HindIII	EcoRI + NotI	-	EcoRI	NotI	HindIII	EcoRI + NotI
Rf band 1		1.1	1.7	1.65	1.65	1.7	1.1	1.65	1.7	1.7	1.75
Fragment 1 length (bp)		17960	6189	6659	6659	6189	17960	6659	6189	6189	5766
Rf band 2		1.9				4.4	1.95				4.35
Fragment 2 length (bp)		4715				604	4425				621
Theoretical fragment length (bp)						599					599

Table 1. Fragment sizes from Restriction Digest Gel Electrophoresis. The resulting gel is shown in Appendix II. This table shows the relative distance travelled (Rf) of the resulting fragments of the restriction digest. The Rf of the DNA ladder (Lane 1) were first calculated and used to construct a standard curve and find a line of best fit. The equation produced, $y = 22677x^{(-2.447)}$, was then used to determine the relative lengths of the resulting bands of each digest. Buffer compatibility was determined from the Thermo Scientific Restriction Enzymes Buffer Activity Chart.

Discussion

In order to determine if Arf6 is a critical component of MCH-mediated actin rearrangements, when Arf6 is inhibited we would expect to see an increase in fibroblast-like cells, as well as a decrease in intermediate and small-round cells in the as well as decreased cell motility.

Fluorescence Stain - The fluorescence stain with NAV-2729, Figure 4B, appeared to confirm our hypothesis by showing a increase in fibroblast-like morphology and an decrease in intermediate cells. However, these changes in cell morphology are also seen in the presence of only DMSO between 0 and 10 minutes of MCH treatment, as shown in figure 4A. Small round cells were sparse, resulting in such a low percentage and such high standard deviation that more trials are needed to obtain accurate data. It is worthy to note that Figure 4 is reflective of only an n=1, and therefore is not statistically significant. In addition to these setbacks, it appeared that the NAV-2729/DMSO solution was not adequately soluble within DMEM-media. A few minutes after addition of the NAV-2729/DMSO solution, a yellow precipitate began to form that not unlike NAV-2729 before being dissolved in DMSO. Incubating in a 37°C water bath and agitation proved ineffective at re-dissolving this precipitate. This led us to question whether or not the cells even had a chance to take up enough, if any, NAV to produce an appreciable effect. Dsouza-Schorey conducted an experiment using NAV-2729 to inhibit Arf6 in uveal melanoma cells [15]. They also used DMSO as a vehicle and showed a considerable difference in cell morphology between the DMSO and NAV treated cells with the NAV treated cells exhibiting increased actin clumping. They determined an IC_{50} values of NAV to be 1.0uM and 3.4uM using fluorometric and orthogonal radiometric ARF6 nucleotide exchange factors, respectively. Our experiment used 10uM NAV and adjusting our own concentrations of NAV would allow a lower overall volume of DMSO to be used.

Scratch wound – There were numerous challenges faces when performing the scratch wound assay the most major of which was cell peeling after creating the initial scratch within the cell monolayer. We believe that this is due to the DMSO vehicle used to dilute NAV-2729. This effect was also exacerbated by frequent agitation of the dishes during transport from the incubator to the microscope for photographing of the scratch. We alleviated this by extending the duration between photographs with appreciable success, however, we did not consider the cells settling after the initial scratch. In our final trial, we successfully obtained photographs of the initial and final scratch over periods of time ranging from 1 hour to 6 hours. Unfortunately, due to cell settling, the final scratch photographs were larger than the initial starting point of the scratch and thus were inconclusive. Cook et al. were able to show that MCH accelerated cell migration [1]. Ideally, if our hypothesis was correct and Arf6 was indeed a critical component of this signaling pathway, then we would have observed an inhibition or reduction of cell migration rate as compared to their results. Overall, our numerous scratch wound assays did not yield any measurable results.

Plasmid verification – The Arf6 plasmids that were sent to us appear to indeed be the plasmids that are shown in Figure 3 based on the data shown in Table 1. We successfully verified the plasmids via the double restriction digest. Unfortunately, due to the lengthy preparation process of these plasmids, we were not able to perform the scratch wound or fluorescence stain with 3T3-L1 cells transfected with the Arf6 plasmids. Our confidence in this method stands as the ARF6 DN T27N plasmid has already been used in 3T3-L1 cells to determine the role of Arf6 on hexose uptake upon stimulation with insulin and endothelin [16].

Conclusion and Future work

Many of the experiments we set out to perform are still incomplete. Due to unforeseen complications and time constraints, we were not able to obtain adequate data to draw any conclusions that are statistically significant. An experiment conducted by Liu et al. successfully inhibited Arf6 protein levels using RNA interference (RNAi) which is a valid and reliable for future Arf6 inhibition. The ARNO and Arf6 plasmids have been prepared and verified, however, we have not yet had a chance to attempt overexpression of the dominant negative forms of ARNO and Arf6. Transfecting the cells with the plasmids would eliminate some of the uncertainties that remain with the use of the NAV drug, such as the formation of a precipitate due to the DMEM media. The use of the plasmids also does not require the use of a vehicle and therefore might aid in obtaining a successful scratch wound assay. Cook et al. reported that PLC activation resulted in a decrease of Class A morphology and thus inhibition of the G_q/PLC pathway is one method to rule out artifacts caused by this pathway. This may also yield a more significant effect upon inhibition of the ARNO/Arf6 pathway; however, it is worthy to note that Dsouza-Schorey's experiment showed a decrease in PLC activity with increased levels of NAV-2729 [15]. Additional analysis and trials are required before any conclusions can be drawn. ARF6 is known to pair with pathways involved in receptor internalization, such as GLUT4 and β Adrenergic receptors , it would be interesting to see whether or not Arf6 has any effect on MCH-mediated internalization of MCHR1 aswell. Further investigation into Arf6 is still of importance due to numerous other studies into its role in membrane trafficking and adipocyte development.

Appendices

I. Scratch method to obtain reference points for image capture of scratch wound developed by Laura Schum. Lines A-D are drawn with a straight edge on the back of an empty culture dish. After cells are grown to confluency, the cell monolayer is scratched adjacent to line D to create a wound that intersects lines A-C. Photographs of the scratch are taken at the intersections and allow for quick and accurate repeat photographs.

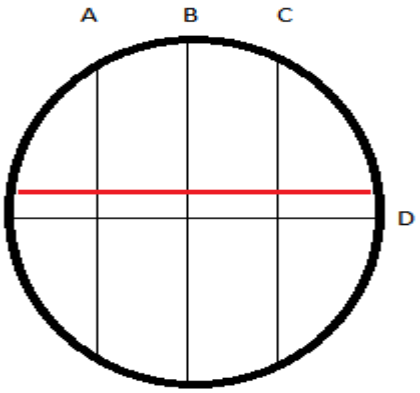

II. Resulting gel from restriction digest. Dropout fragments from double digest using ECORI and NotI are shown boxed in white. Lane 1 shows the 1Kb DNA ladder used to determine the relative fragment sizes. The contents of each lane are shown in Table 1.

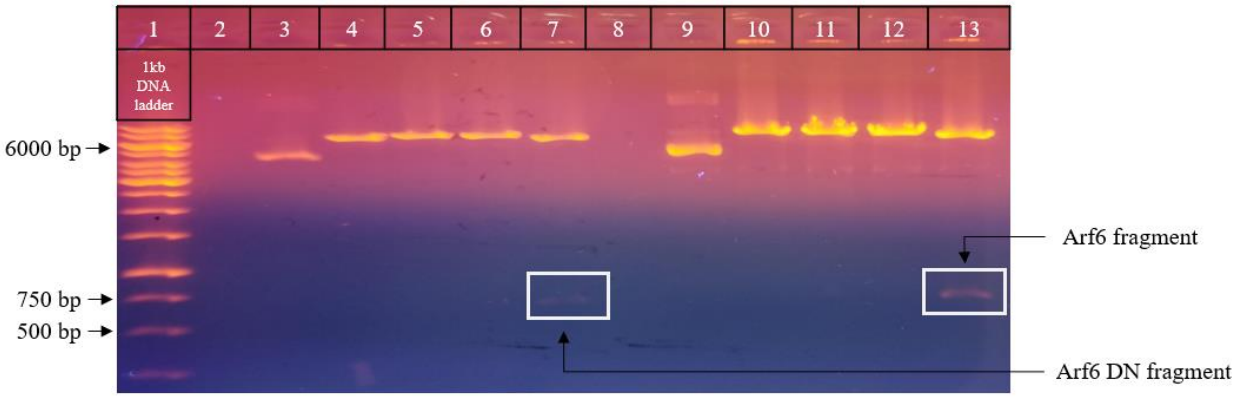

Bibliography

1. Cook, L. B., Shum, L., & Portwood, S. (2010). Melanin-concentrating hormone facilitates migration of preadipocytes. *Molecular and Cellular Endocrinology*, *320*(1-2), 45–50. doi: 10.1016/j.mce.2010.02.009
2. Ludwig DS, Tritos NA, Mastaitis JW, Kulkarni R, Kokkotou E, Elmquist J, Lowell B, Flier JS, Maratos-Flier E. Melanin-concentrating hormone overexpression in transgenic mice leads to obesity and insulin resistance. Journal of Clinical Investigation. 2001;107(3):379–386. doi:10.1172/jci10660
3. Ghoussaini M, Vatin V, Lecoeur Cécile, Abkevich V, Younus A, Samson C, Wachter C, Heude B, Tauber Maïté, Tounian P, et al. Genetic Study of the Melanin-Concentrating Hormone Receptor 2 in Childhood and Adulthood Severe Obesity. The Journal of Clinical Endocrinology & Metabolism. 2007;92(11):4403–4409. doi:10.1210/jc.2006-2316
4. Schou KB, Pedersen LB, Christensen ST. Ins and outs of GPCR signaling in primary cilia. EMBO reports. 2015;16(9):1099–1113. doi:10.15252/embr.201540530
5. Donaldson JG. Multiple Roles for Arf6: Sorting, Structuring, and Signaling at the Plasma Membrane. Journal of Biological Chemistry. 2003;278(43):41573–41576. doi:10.1074/jbc.r300026200
6. Dunphy JL, Moravec R, Ly K, Lasell TK, Melancon P, Casanova JE. The Arf6 GEF GEP100/BRAG2 Regulates Cell Adhesion by Controlling Endocytosis of β1 Integrins. Current Biology. 2006;16(3):315–320. doi:10.1016/j.cub.2005.12.032
7. Furman C, Short SM, Subramanian RR, Zetter BR, Roberts TM. DEF-1/ASAP1 Is a GTPase-activating Protein (GAP) for ARF1 That Enhances Cell Motility through a GAP-

dependent Mechanism. Journal of Biological Chemistry. 2001;277(10):7962–7969. doi:10.1074/jbc.m109149200

8. Claing A, Chen W, Miller WE, Vitale N, Moss J, Premont RT, Lefkowitz RJ. β-Arrestin-mediated ADP-ribosylation Factor 6 Activation and β2-Adrenergic Receptor Endocytosis. Journal of Biological Chemistry. 2001;276(45):42509–42513. doi:10.1074/jbc.m108399200
9. Frank S, Upender S, Hansen SH, Casanova JE. ARNO Is a Guanine Nucleotide Exchange Factor for ADP-ribosylation Factor 6. Journal of Biological Chemistry. 1998;273(1):23–27. doi:10.1074/jbc.273.1.23
10. Kang DS, Tian X, Benovic JL. β-Arrestins and G Protein-Coupled Receptor Trafficking. Methods in Enzymology G Protein Coupled Receptors - Trafficking and Oligomerization. 2013:91–108. doi:10.1016/b978-0-12-391862-8.00005-3
11. Liu Y, Zhou D, Abumrad NA, Su X. ADP-ribosylation factor 6 modulates adrenergic stimulated lipolysis in adipocytes. American Journal of Physiology-Cell Physiology. 2010;298(4). doi:10.1152/ajpcell.00541.2009
12. Pissios P, Trombly DJ, Tzameli I, Maratos-Flier E. Melanin-Concentrating Hormone Receptor 1 Activates Extracellular Signal-Regulated Kinase and Synergizes with Gs-Coupled Pathways. Endocrinology. 2003;144(8):3514–3523. doi:10.1210/en.2002-0004
13. Lounsbury K. Signal Transduction and Second Messengers. Pharmacology. 2009:103–112. doi:10.1016/b978-0-12-369521-5.00006-3
14. Sit S-T, Manser E. Rho GTPases and their role in organizing the actin cytoskeleton. Journal of Cell Science. 2011;124(5):679–683. doi:10.1242/jcs.064964

15. Dsouza-Schorey C. Faculty Opinions recommendation of ARF6 Is an Actionable Node that Orchestrates Oncogenic GNAQ Signaling in Uveal Melanoma. Faculty Opinions – Post-Publication Peer Review of the Biomedical Literature. 2016 Nov. doi:10.3410/f.726403508.793520738
16. Lawrence JTR, Birnbaum MJ. ADP-Ribosylation Factor 6 Delineates Separate Pathways Used by Endothelin 1 and Insulin for Stimulating Glucose Uptake in 3T3-L1 Adipocytes. Molecular and Cellular Biology. 2001;21(15):5276–5285. doi:10.1128/mcb.21.15.5276-5285.2001